Nigerian Journal of Environmental Sciences and Technology (NIJEST)

www.nijest.com

ISSN (Print): 2734-259X | ISSN (electronic): 2734-2603

Vol 6, No. 1 March 2022, pp 180 - 192

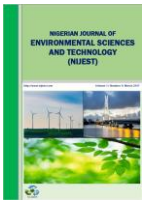

3D City Model from LiDAR of Akoka, Lagos Using Geographical Information Technique

Makinde E. O.[1,]* and Onaneye A.O.[2]

[1,2]Department of Surveying and Geoinformatics, Faculty of Engineering, University of Lagos, Akoka, Lagos State, Nigeria

Corresponding Author: *eomakinde@unilag.edu.ng

https://doi.org/10.36263/nijest.2022.01.0292

ABSTRACT

3D city models are now widely adapted globally and since Lagos state is fast developing into a megacity, there is the need to have proper 3D city visuals. This study therefore created and visualized a 3D building model from LiDAR and orthophoto data of Akoka in Lagos State using geographical information techniques. A recently digitized Google Earth satellite image of the study area was compared with the Orthophoto to identify major changes in the area. The LiDAR point cloud data was classified using the automatic classification of LiDAR data method and then subsequently classified into buildings, vegetation, water body, grounds and roads. Elevation models such as Digital Terrain Model (DTM), Triangular Irregular Network (TIN) surface model and Digital Surface Model (DSM) were generated from the processed LiDAR data. Furthermore, maximum likelihood algorithm was used to classify the LiDAR image. And then accuracy assessment technique performed on the classified image. The result of the accuracy assessment indicated that the overall classification was 66.00% while the overall kappa statistics was 0.5677. This study concluded that the application of geographical information technique to LiDAR images can be used to assess, visualize and model 3D cities which can be very effective and useful in advancing the geospatial industry and enhancing urban planning for smart cities.

Keywords: LiDAR, Orthophotos, Smart Cities, City Geographic Markup Language, DTM

1.0. Introduction

In recent times, the rapid growth of three dimensional (3D) city models have turned to be one of the most sort after representation of an area creating a real time visualization for development in urban planning, urban landscapes, real estate management etc. 3D-city model (3D-CM) can be referred to as a special computer representation of all fixed objects (buildings, vegetation, traffic ways and waterways) within an area which contains all the information necessary to view each object from all sides and the main characteristics to make it recognizable (Sohn and Dowman, 2002). 3D urban models are broadly utilized in urban planning such as the set-up of media transmission systems, utility administrations observing, air contamination control, and so forth. The creation of an urban model requires object extraction, which distinguishes the object of intrigue and concentrates its geometric limit from remotely detected information (Sohn and Dowman, 2002). Studies have been done on the extraction of buildings in urban areas from the combination of image and light detection and ranging (LiDAR) datasets (Halla and Brenner, 1999; Zhou and Neumann, 2008) and even the fusion of LiDAR and image (Rottensteiner *et al.*, 2004). Sensors such as high-resolution imager, synthetic aperture radar (SAR) and LiDAR, produces good images that have turned out to be pertinent. For example, semi-automated and automated 3D building models with larger amounts of detail and exactness can be created from these sensors which are plausible. The incorporated utilization of the information given by two diverse sensor types empowers us to stay away from the shortcoming purposes of either sensor. This is because the combination of two sensors yields an improved output.
The acronym, LiDAR, means Light Detection and Ranging and it is a method in remote sensing that uses light in the form of a pulsed laser to measure ranges (variable distances) to the Earth. LiDAR uses laser to measure features. These light pulses combined with other data recorded by the airborne

system to generate precise, three-dimensional information about the shape of the Earth and its surface characteristics (Tao and Hu, 2001). LiDAR and aerial picture are two integral information sources to distinguish and extract building limits. The LiDAR system is recognized as state-of-the-art tool which enables the generation of high resolution, highly precise, and large-scale elevation information (Baltsavias, 1999). The development of airborne laser scanning goes back to the 1970s (Baltsavias *et al*., 1995). By emitting a laser pulse and precisely measuring the return time to the source the range can be calculated using the value for the speed of light. In the late-80s kinematic GPS provided the necessary centimeter level positioning accuracy required for high performance LiDAR. The systems required ultra-accurate clocks for timing the return and Inertial Measurement Units (IMU) for capturing the orientation of the scanner (Wehr and Lohr, 1999).

According to Lindenberger (1993), mathematical morphology in the field of image processing of LiDAR data, is used to describe the spatial structure based on a set of morphological operators. A morphological operator changes an image into regions of homogeneity, where structures of interest are emphasized. To start this processing, an operator and potential regions are essential. The seed regions are first detected by the lowest (minimum elevation) points within each structure window moving along a profile. Then the terrain regions are extended to neighbouring points if the elevation differences are small (Lindenberger, 1993). The neighbourhood can be defined either along LiDAR profiles (Shan and Sampath, 2005), in a multi-directional fashion in rasterized height image (Meng *et al.*, 2009), or through neighbouring points within a certain distance (Vosselman, 2000). Zhang and Chen (2003) proposed a progressive morphological filter by gradually enlarging the window size. With iteratively increasing window size, the height difference is calculated between surfaces after morphological opening. Points within a certain height difference are identified from the terrain surface. Chen *et al.* (2007) extended adaptive morphological filtering by first performing an opening operation to remove tree points via a relatively small window. Then, building points are filtered with a larger window in a similar way to the Zhang and Chen (2003) approach. Triangulation meshes generated from point clouds are also a popular input format for the processing of LiDAR datasets (Tse *et al.*, 2005). Meshes consist of a set of triangles formed by connecting of their common corners or edges to provide connectivity information. Nevertheless, geometric features from spurious triangles are often unreliable due to the presence of noise (Maas and Vosselman, 1999). Besides, triangulation meshes are derived from point clouds, so processing directly on point cloud is preferable. The TIN model represents a surface as a set of contiguous, non-overlapping triangles. Within each triangle the surface is represented by a plane. The triangles are made from a set of points called mass points.
Digital terrain model (DTM) and digital surface model (DSM) can be created from the LiDAR data after filtering. DTM is the description of the terrain surface using a set of heights over 2D points residing on a reference surface. It approximates a part or the whole of the continuous terrain surface by a set of discrete points with unique height values over 2D points. Heights are in approximation vertical distances between terrain points and some reference surface (e.g., mean sea level, geoid and ellipsoid) or geodetic datum (Meng *et al.*, 2010). There are several categories of DTM generation algorithms (Meng *et al.*, 2010). Kraus and Pfeifer (1998) proposed a DTM generation algorithm based on robust linear prediction, which has been widely accepted by researchers. Firstly, a rough estimation of the terrain surface is computed using some control ground points (usually acquired using the lowest point for each cell). Kobler *et al.* (2007) proposed a repetitive interpolation method. This approach attempts to filter non-ground points through several steps. First, some traditional methods are employed to preliminarily remove most outliers and non-ground returns. By comparing the distribution of the estimated elevation with the global mean offset, the remaining non-ground points can be effectively filtered. Chen *et al.* (2006) used an iterative terrain recovery approach for DTM generation.

Digital surface model (DSM) is an elevation model that includes the tops of everything, including buildings, treetops, and ground where there is nothing else on top of it (Amhar *et al.*, 1998). The generation of accurate orthophotos based on the use of DSM to model the ground geometry was first proposed by Amhar *et al.* (1998) under the term "True-Ortophoto", and then implemented in different commercial photogrammetric packages. From a theoretical point of view, the generation of a True-Orthophoto does not significantly differ from that of classical orthophotos (Amhar *et al.*, 1998). The most complex issue to cope with is related to what is called roof modeling according to Schickler

(1998). Schickler (1998) stated that if indeed, the goal is to generate a high resolution True-Orthophoto® and the DSM features has a low planimetric resolution, information about where the roof border of a building is located might be lacking. This is because the algorithm does not know if a pixel of the image represents a piece of terrain or the roof of a building (Schickler, 1998). However, most methodologies for a programmed age of 3D city models in writing depend on an amazing DSM (Amhar *et al.,* 1998). For instance Brenner (2000) portrays completely programmed remaking frameworks dependent on an amazing laser DSM. Additionally, Rottensteiner (2004), utilize top notch laser DSMs and aerial imagery for automatic extraction of building roofs in densely built-up areas. Khoshelham *et al.* (2005) applied a split-and-merge technique on a DSM guided image segmentation technique for automatic extraction of roof planes.

LiDAR data can be classified and the classification approach detects the ground points using certain operators designed based on mathematical morphology (Lindenberger, 1993; Vosselman, 2000) or terrain slope (Axelsson, 1999) or local elevation difference (Wang and Tseng, 2004). It has been reported that refined classification approach uses Triangulated Irregular Network (TIN) data structure (Axelsson, 2000; Vosselman and Mass, 2001) and iterative calculation (Axelsson, 2000; Sithole, 2001) to consider the discontinuity in the LiDAR data or terrain surface. Algorithms for classifying LiDAR point clouds can be grouped into two categories based on used data type: point clouds and raster range image. The first kind of algorithm is used on point clouds of LiDAR directly while the second kind works with raster images, to enable the irregularly distributed LiDAR point cloud to be gridded (Bao *et al.,* 2008). The features of all points in the LiDAR point cloud are used in automatic point-based classification applications and appropriate parameters of these features are usually determined as a result of training steps according to the targeted classes in the classification stage (Kim and Sohn, 2010; Mallet *et al.,* 2011; Kim and Sohn, 2013, Yastikli and Cetin, 2016). In characterization ventures of the LiDAR point mists, each point is appointed to the significant classes, for example, ground, vegetation, working as per the qualities of the LiDAR information (Yastikli and Cetin, 2016). Most of the time LiDAR point cloud data transformed into image data, so the traditional pixel based classification or the object-based segmentation and classification techniques can be directly used for LiDAR data classification (Gu *et al.,* 2016). Thus, this study acquired secondary images from the Office of the Surveyor General of Lagos State, Nigeria, processed them and analysed them using the traditional pixel based classification method of the maximum likelihood algorithm.

2.0. Methodology

2.1. Study area

Akoka is a suburb of Yaba local government in Lagos State. It is a developing urban area known to be the hub of major educational institutions such as the University of Lagos and Federal College of Education (Technical) and also holds various commercial activities and numerous residential buildings. Akoka is located between latitude 03.2343°E and 0.34554°E and 06.2135°N and 06.4323°N. Akoka has a tropical climate with an average temperature of 27.0 °C and average annual rainfall is 1693 mm. Figure 1 shows the Google Earth image of the study area.

Figure 1: Google Earth Image showing Akoka and environs

2.2. Data source

This study used LiDAR and Orthophoto data of 2009 acquired from the Office of State Surveyor General (OSSG), Lagos State with a spatial resolution of 20cm. In addition, Google Earth images were acquired from Google Earth Pro, using Smart GIS Map Editor and GPS Tracking 2018 software to download the data.

2.3. Data processing

The Goggle Earth images were enhanced and features such as roads and buildings were extracted by digitizing. Since LiDAR is a point cloud data, it was processed to eliminate unwanted noise by automatic classification of noise using the maximum allowed variance from local average to 3 standard deviations (Figure 2).

This allows us to determine the number of standard deviation from the mean to identify as noise based on this point cloud data. The mark noise outside elevation range was set to 0 -25 based on sea level and maximum height of our data. And then likely noise points from points that are already classified were identified (Figure 2a). Figure 2b shows the profile graph after the noise elimination for the LiDAR data. The LiDAR data was then filtered (Figure 2c) and auto classification of ground points and non-ground points (Building/Tree) were performed.

Building and tree features were extracted from the LiDAR data using a point spacing resolution of 0.5. This value was set in order to be able to identify the building features. Other parameters set are extract building footprints, create separate 3D areas for different roof pieces if possible by setting the max co-planar angle difference to 25 degrees and the maximum distance from adjacent plane to 0.25 meters. The simplification multiplier for soothing building was set to 4 to remove vertices and create simple fairly square or rectangular footprints. For the tree features, the minimum tree height and spread were set to 0.2 meters and 0.5 meters respectively. A TIN surface ground model, DTM and DSM were then created.

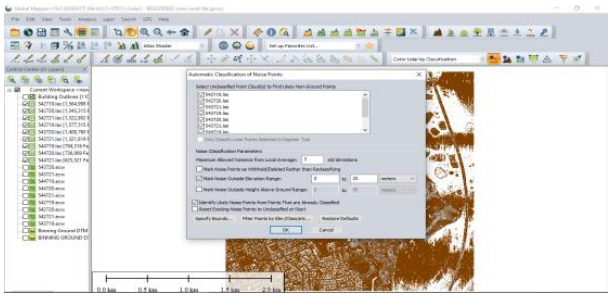

(a) Step for auto-classification of noise

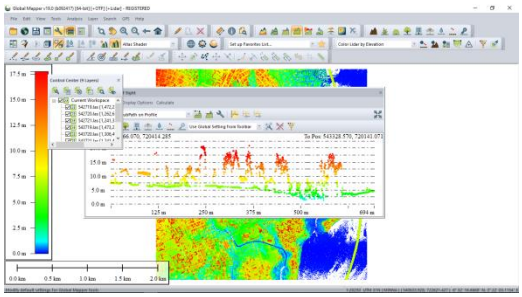

(b) Step for Sub-path Profile

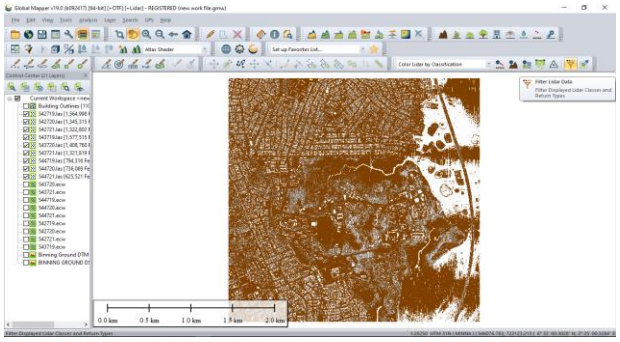

(c) Filtering Noise Data in the LiDAR

Figure 2: LiDAR data being processed

2.4. Image classification

The processed LiDAR was brought into ERDAS Imagine software to perform the maximum likelihood classifier algorithm. Training samples were selected covering six classes identified adopted from the Anderson classification scheme as land cover classes and used to classify the image as reported by Fisher (2010); Makinde and Oyelade (2019). The maximum likelihood classifier algorithm was used to classify the image. This algorithm assumes that the statistics for each class in each band are normally distributed and calculates the probability that a given pixel belongs to a specific class. Unless a probability threshold is selected, all pixels are classified. Each pixel is assigned to the class that has the highest probability (that is, the maximum likelihood). If the highest probability is smaller than a threshold specified, the pixel remains unclassified. The equation for the maximum likelihood/Bayesian classifier is as follows (ERDAS, 2006):

$$D = \ln(ac) - [0.5\ln(|Covc|)] - [0.5(X - M_c)T(Covc - 1)(X - M_c)] \quad (1)$$

Where:

D = Weighted distance (likelihood)
c = A particular class
X = The measurement vector of the candidate pixel
Mc = The mean vector of the sample of class c
ac = Percent probability that any candidate pixel is a member of class c (defaults to 1.0, or is entered from a priori knowledge)
Covc = The covariance matrix of the pixels in the sample of class c
|Covc| = Determinant of Covc (matrix algebra)
Covc-1 = Inverse of Covc (matrix algebra)
ln = Natural logarithm function
T = Transposition function (matrix algebra)

The inverse and determinant of a matrix, along with the difference and transposition of vectors, would be explained in a textbook of matrix algebra. The pixel is assigned to the class, c, for which D is the lowest.

2.5. Image post-processing

The image post-processing performed was the Accuracy assessment. This is to check the accuracy of the recently classified image to know the extent of accuracy of the classification given in percentage. The accuracy assessment was done using ERDAS Imagine 2014. The stratified sampling technique used on the classified image to acquire the error matrix.

$$N = (\sum_{i=1}(Wi - Si) \div So)\text{^}2 \quad (2)$$

Where:
Wi = mapped area portion of class 1;
Si = standard deviation of stratum i;
So = expected standard deviation of overall accuracy;
c = total number of classes
It is a standard to use So = 0.01

3.0. Results

3.1. Digitized outline of Buildings and Roads in Akoka

The buildings and roads in the Akoka environment were digitzed to provide a defined outline of the buildings and roads creating shapefile “POLYGON” and naming it “Buildings” to represent the buildings and shapefile “POLYLINE” and naming it “Roads” to represent the roads.

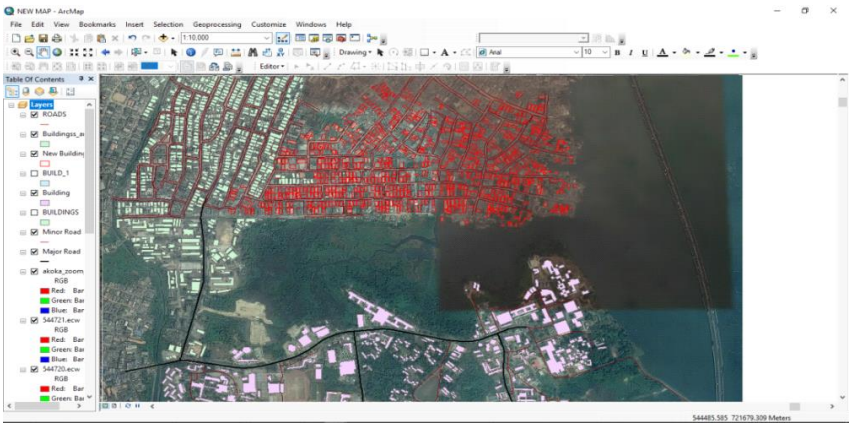

Figure 3: Digitized map of Akoka

From Figure 3, the features (Buildings and roads) are digitized to show their outlines for easier understanding of the area and identification of individual features.

3.2. Classified LiDAR data

The Las data file was classified automatically into three aspects which are: auto classification of noise points, auto classification of ground points and auto classification of non-ground points (Building/Tree) as seen in Figures 4-6.

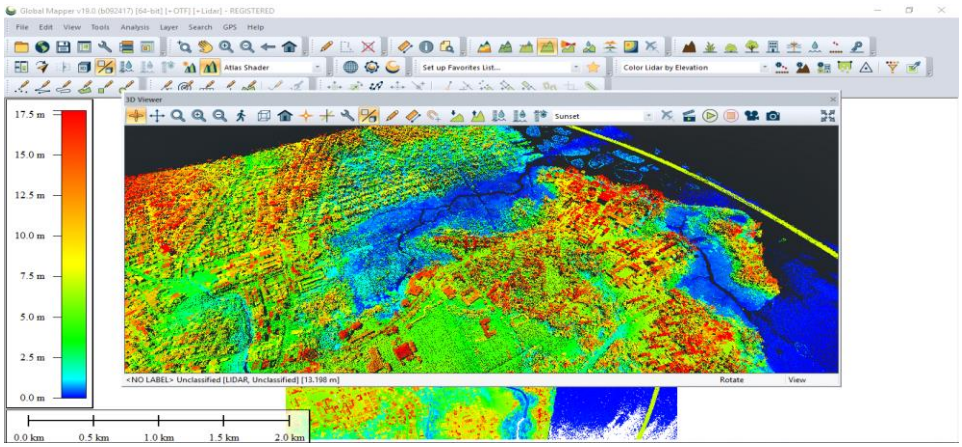

Figure 4: LiDAR data after auto-classification of noise points in 3D view

The procedure was done to eliminate noise within the LiDAR data so when during the classification they won't be recognized as valid points.

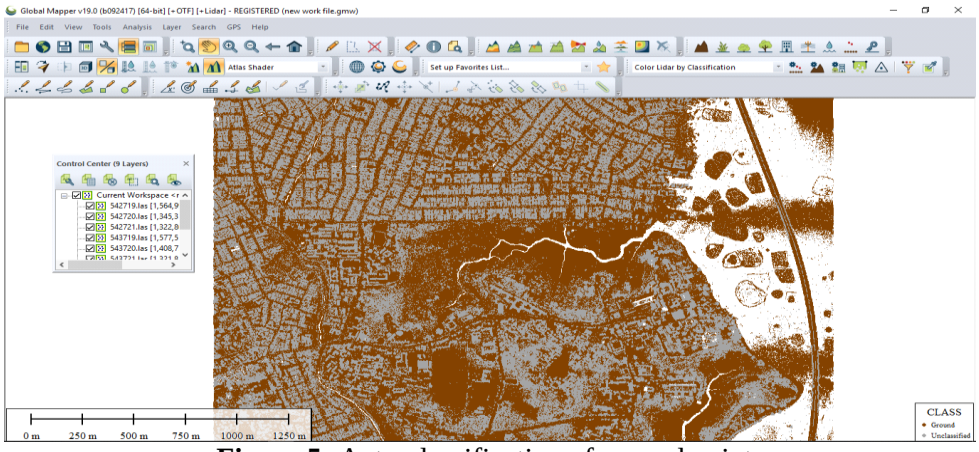

Figure 5: Auto-classification of ground points

This procedure was done to classify the non-ground points between a certain range as mentioned above, before classification of non-ground points (buildings, vegetation, etc.)

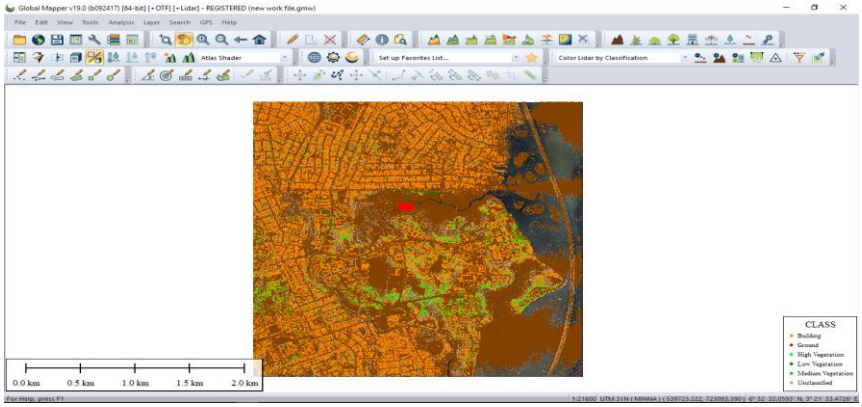

Figure 6: Auto-classification of non- ground points

This result shows us the classification of the LiDAR data after automatic classification of non-ground points (buildings, vegetation, etc.).

3.3. Digital Elevation Models

3.3.1. TIN Surface Ground Model

The Triangulation Network surface model was generated to produce a surface model of Akoka area showing the elevation of buildings and trees in that area (Figure 7).

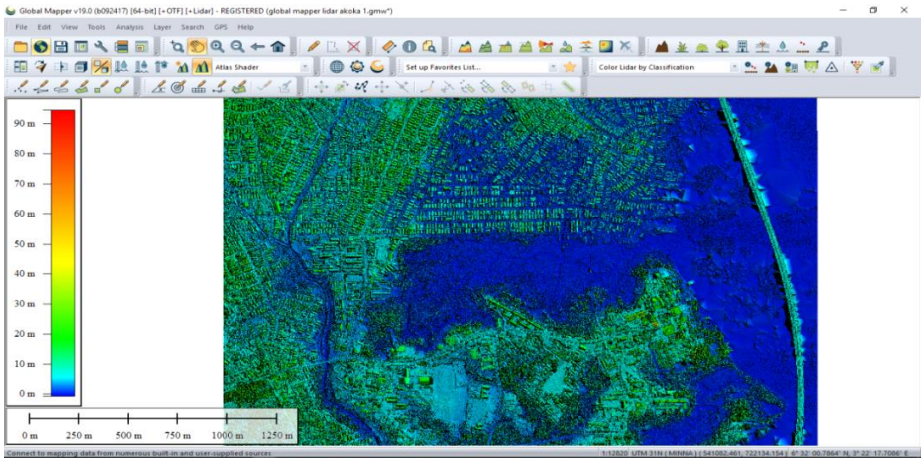

Figure 7: Generated TIN Surface Ground Model

3.3.2. A digital surface map of Akoka

The Digital surface model shows the Earth's surface and the elevation of the reflective surfaces of trees, building and roads above the bare earth (Figure 8).

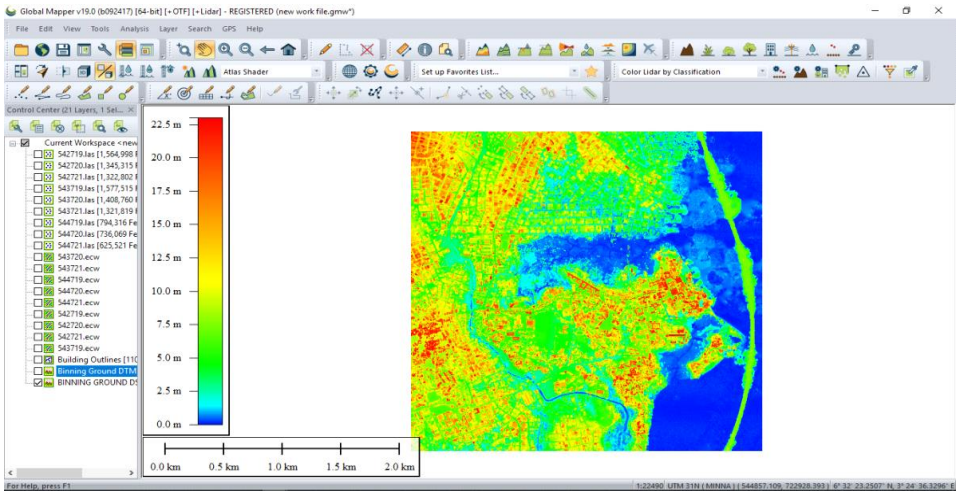

Figure 8: Generated Digital Surface Model

3.3.3. A Digital Terrain Map of Akoka

The Digital Terrain model represents the terrain and ground topography of the study area (Figure 9).

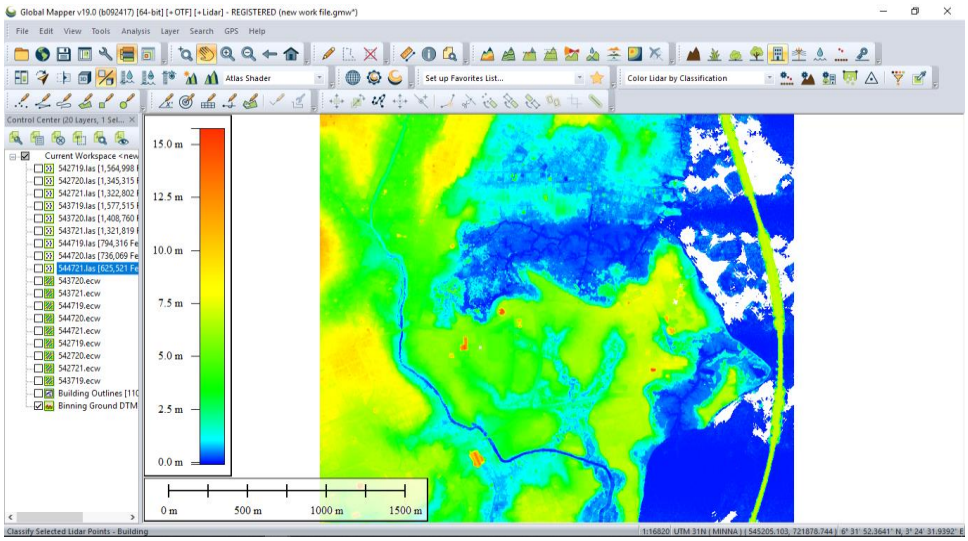

Figure 9: Generated Digital Terrain Model

3.4. Image Classification and Accuracy Assessment

The classification of the image of Akoka is shown in Figure 10.

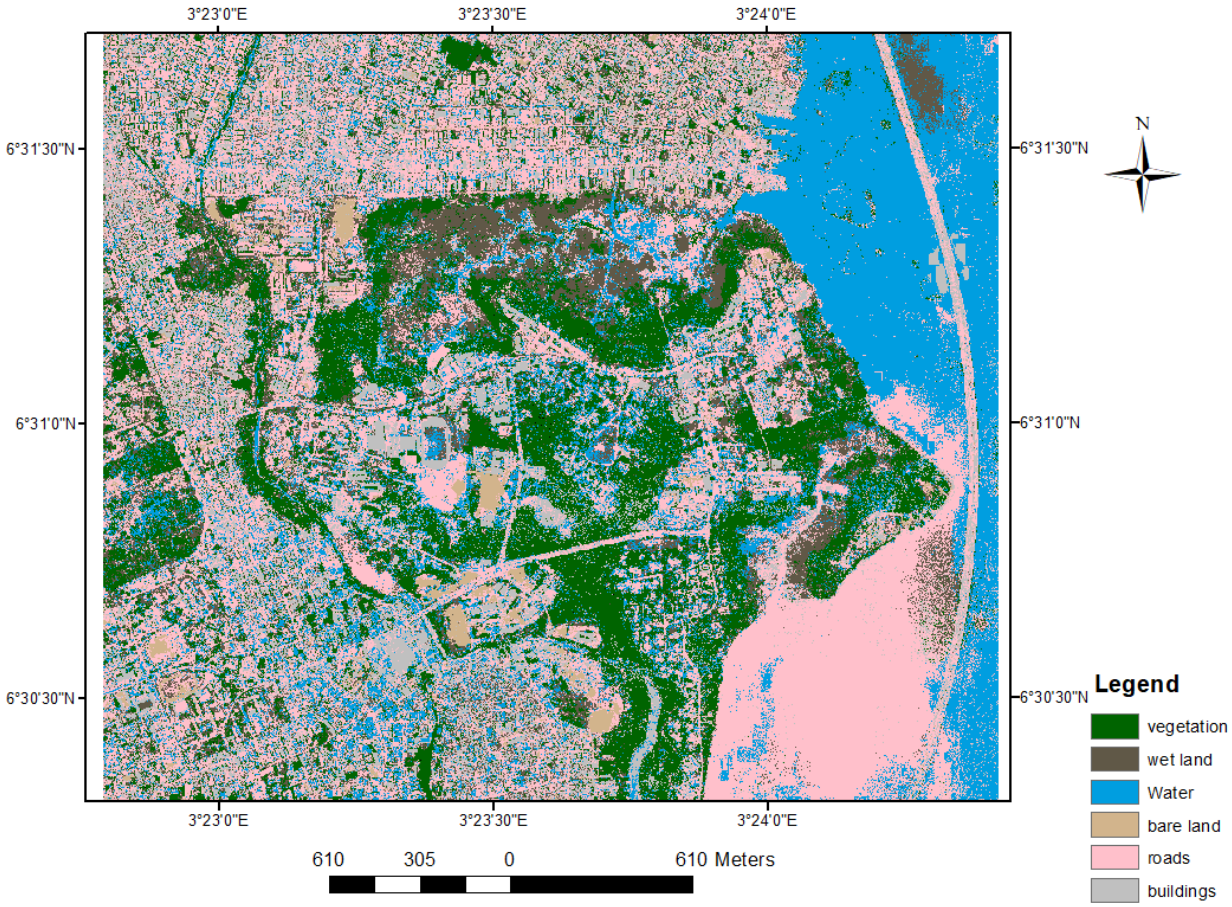

Figure 10: Classified image of Akoka

3.5. Accuracy assessment

Accuracy assessment shows us the percentage of how accurate the supervised classification is with the use of 100 random points across the classified image which was done automatically in ERDAS Imagine. The overall classification accuracy is 66.00% and the overall kappa statistics is 0.5677.

4.0 Discussion

The map digitization was done in sections and merged together to form the digitized map. The digitized map gives credible information about Akoka by showing the various building footprints as well as the footprints of the roads in their various shapefiles. The building Shapefile type was "Polygon". From the result we can see that different buildings represented with the polygon shapefile describe their outline as well as show their positions.

The LiDAR was classified into Non-ground points and Ground points of which they are represented uniquely according to their classes. The ground point LiDAR classification was done to classify the points within a specific elevation range as ground points, so we can identify which LiDAR points are ground points (roads & bare grounds). The non-ground points classification was also done to classify points within a specific elevation range to be classified as non-ground points (trees, buildings, power lines and etc.). The result obtained aids building extraction.

Digital Elevation models are important in the aspect of three dimensional model generation because it has to be done using a z value. The elevation models are being generated from the LiDAR data using Global Mapper v19.0 to automatically generate the models: TIN, DEM, DSM. The TIN surface model generated is a DEM that uses continuous surface consisting entirely of triangular facets to create elevations and represent the physical land surface and water bodies in three dimensions. The DTM generated is a vector data set composed of regularly spaced points and natural features such as ridges and breaklines, creating greater accuracy as it contains additional information defining terrain in areas where LiDAR data alone is unable to do the job effectively. This terrain information can be used in various geo-related applications such as hydrology, natural hazard process modeling and geomorphological mapping. The DSM generated captures the natural and built features on the Earth's surface which represents the height, above mean sea level, of the features (e.g. crops, buildings, trees, etc.) This agrees with the study of Zhou and Newman (2008).

The classification of Image was done using ERDAS Imagine software 2014 to perform a supervised classification on the mosaic Orthophoto which is a secondary data. The type of supervised classification method which was used was maximum likelihood. Spectral signature was used for the classification where a polygon was created to represent various Area of Interests (AOIs) which were grouped into classes and similar classes with their spectral signature are merged. After the classification of the image, a further image post-process method is applied which is accuracy assessment. The accuracy assessment is done to check the percentage of accuracy of the operation. Accuracy assessment helps to understand the classification and know the error level of the classification by comparing the class value with the reference data. The accuracy assessment for this study returned 66%. This is probably because of what is called spatial and spectral tradeoff of images. Although the image used in this study has more spatial details, it has lower class separability when training its classifiers and therefore will yield a lower accuracy assessment than when compared to say, a Landsat image as noted by Makinde *et al.* (2016).

5.0. Conclusions

This study assessed the LiDAR point cloud data and high-resolution satellite imagery of Akoka in Lagos. The data were processed, classified and a 3D model generated. The derived result of this research depicts that automated 3D building models can be produced effectively by utilizing raw LiDAR point cloud data. The obtained 3D building models can be utilized in various applications such as 3D city displaying, ecological recreation, media transmission and versatile route. Although, a LiDAR image data of any part of Nigeria is not easy to come by, this study was able to access LiDAR data and use it to assess the Akoka area of Lagos in 3D. This study concluded that image classification and various elevation types can be extracted from a LiDAR data which serves as input into a decision support system (DSS) of Lagos State.

References

Amhar, F., Jansa, J. and Ries, C. (1998). The Generation of the True-Orthophotos Using a 3D Building Model in Conjunction With a Conventional DTM, *The Int. Archive of Phot. and R.S.,* 32(4), pp. 16-22, Stuttgart, Germany.

Axelsson, P. (1999). Processing of laser scanner data-algorithms and applications. *ISPRS Journal of Photogrammetry and Remote Sensing,* 54, pp. 138–147.

Axelsson, P. (2000). DEM generation from laser scanner data using adaptive TIN models. *International Archives of Photogrammetry, Remote Sensing and Spatial Information Sciences,* 33, pp. 110–117.

Bao, Y., Li, G., Cao, C., Li, X., Zhang, H., He, Q., et al. (2008). Classification of LiDAR Point Cloud and Generation of DTM from LiDAR Height and Intensity Data in Forested Area. In: *The International Archives of the Photogrammetry, Remote Sensing and Spatial Information Sciences*, Beijing, China, Vol. XXXVII, Part B3b.

Baltsavias, E., Mason, S. and Stallmann, D. (1995). Use of DTMs=DSMs and orthoimages to support building extraction. In: Gruen, A., Ku¨bler, O., Agouris, P. (Eds.), Automatic Extraction of Man-Made Objects from Aerial and Space Images. Birkha¨user, Basel, pp. 199–210.

Baltsavias, E.P. (1999). A comparison between photogrammetry and laser scanning. *ISPRS Journal of Photogrammetry and Remote Sensing*, 54, pp. 83–94.

Brenner, C. (2000). Towards fully automatic generation of city models. *International Archives of Photogrammetry, Remote Sensing and Spatial Information Sciences*, 33, pp. 85–92.

Chen Q., Wang H., Zhang H., Sun M. and Liu X. A. (2006). Point cloud filtering approach to generating DTMs for steep mountainous areas and adjacent residential areas. *Remote Sens.* 8 (71), doi: 10.3390/rs8010071.

Chen, Q., Gong, P., Baldocchi, D. and Xie, G. (2007). Filtering airborne laser scanning data with morphological methods. *Photogrammetric Engineering and Remote Sensing,* 73, pp. 175–185.

ERDAS, (2006). ERDAS Imagine V9.1. ERDAS, Atlanta, GA, USA.

Fisher, P.F. (2010). Remote sensing of land cover classes as type 2 fuzzy sets. *Remote Sens. Environ*. 114, pp. 309–321.

Gu, Y., Wang, Q. and Xie, B. (2016). Multiple kernel sparse representation for airborne LiDAR data classification. *IEEE Trans. Geosci. Remote Sens*. 2016, 1–21.

Haala, N. and Brenner, C. (1999). Extraction of buildings and trees in urban environments. *ISPRS Journal of Photogrammetry & Remote Sensing*, 54, pp. 130-137.

Kobler, A., Pfeifer, N., Ogrinc, P., Todorovski, L., Ostir, K. and Dzeroski, S. (2007). Repetitive interpolation: A robust algorithm for DTM generation from aerial laser scanner data in forested terrain. *Remote Sens. Environ*. 108, pp. 9–23. doi: 10.1016/j.rse.2006.10.013

Khoshelham, K., Li, Z. and King, B. (2005). A split-and-merge technique for automated reconstruction of roof planes. *Photogrammetric Engineering and Remote Sensing*, 71(7), pp. 855–862.

Kim, H. B. and Sohn, G. (2010). 3D Classification of Power-Line Scene From Airborne Laser Scanning Data Using Random Forests, *ISPRS Archives*, September 1-3, Saint-Mandé, France, 38(3A), pp. 126-132.

Kim, H. B. and Sohn, G. (2013). Point-Based Classification of Power Line Corridor Scene Using Random Forests, *Photogrammetric Engineering and Remote Sensing*, 79, pp. 821–833.

Kraus, K. and Pfeifer, N. (1998). Determination of terrain models in wooded areas with airborne laser scanner data. *ISPRS Journal of Photogrammetry and Remote Sensing*, 53, pp. 193–203.

Lindenberger, J. (1993). Laser-Profilmessungen zur topographischen el ndeaufnahme. PhD thesis.

Maas, H. and Vosselman, G. (1999). Two algorithms for extracting building models from raw laser altimetry data. *ISPRS Journal of Photogrammetry and Remote Sensing*, 54, pp. 153–163.

Makinde, E.O. and Oyelade, E. O. (2019). Land Cover Mapping using Sentinel-1 SAR and Landsat 8 imageries of Lagos State for 2017. *Environmental Science and Pollution Research*, 1-9. Springer. https://doi.org/10.1007/s11356-019-05589-x

Makinde, E. O., Salami, A. T., Olaleye, J. B. and Okewusi, O. C. (2016). Object Based and Pixel Based Classification Using RapidEye Satellite Imagery of ETI-OSA, Lagos, Nigeria. *Geoinformatics FCE CTU*, 15(2), 59. Department of Geomatics, Faculty of Civil Engineering, Czech Technical University in Prague. Indexed Platform: CrossRef. DOAJ, doi:10.14311/gi.15.2.5.

Mallet, C., Bretar, F., Roux, M., Soergel, U., Heipke, C., (2011). Relevance Assessment of Full-Waveform Lidar Data for Urban Area Classification, *ISPRS Journal of Photogrammetry and Remote Sensing*, 66(6): 71–S84.

Meng, X., Currit, N. and Zhao, K. (2010). Ground Filtering Algorithms for Airborne LiDAR Data: A Review of Critical Issues. *Remote Sens*. 2, pp.833–860. doi: 10.3390/rs2030833.

Meng, X., Wang, L., Silván-Cárdenas, J.L. and Currit, N. (2009). A multi-directional ground filtering algorithm for airborne LiDAR. *ISPRS Journal of Photogrammetry and Remote Sensing*, 64, pp. 117–124.

Rottensteiner, F., Trinder, J., Clode, S. and Kubik, K. (2004). Fusing airborne laser scanner data and aerial imagery for the automatic extraction of buildings in densely built-up areas. In: Proc. ISPRS Twentieth Annual Congress, Istanbul, Turkey, pp. 512– 517.

Schickler W. (1998). Operational Procedure for Automatic True Orthophoto Generation. *IAPRSSIS*, 32(4), pp.527532.

Shan, J. and Sampath, A. (2005). Urban D M generation from raw iDAR Data : a labeling algorithm and its performance. *Photogrammetric Engineering & Remote Sensing* 71, pp. 217–226.

Sithole, G. (2001). Filtering of laser altimetry data using a slope adaptive filter. Int. Arch. Photogramm. *Remote Sens. Spat. Inf. Sci*. 34, pp. 203–210.

Sohn, G. and Dowman, I. (2002). Terrain surface reconstruction by the use of tetrahedron model with the MDL criterion. *International Archives of Photogrammetry and Remote Sensing* 34, pp. 336–344.

Tao, C. V. and Hu, Y. (2001). A comprehensive study of the rational function model for photogrammetric processing. *Photogrammetric Engineering & Remote Sensing*, 67(12):1347–1357.

Tse, R., Gold, C.M. and Kidner, D.B. (2005). Building reconstruction using LiDAR data.ISPRS Workshop on Updating Geo-spatial Databases with Imagery & The 5th ISPRS Workshop on DMGISs 121–126.

Vosselman, G. (2000). Slope based filtering of laser altimetry data. *International Archives of Photogrammetry, Remote Sensing and Spatial Information Sciences*, 33, pp. 935–942.

Vosselman, G. and Maas, H.G. (2001). Adjustment and filtering of raw laser altimetry data. In: OEEPE Workshop on Airborne Laser Scanning and Interferometric SAR for Detailed Digital Elevation Models, Stockholm, Sweden, 40, pp. 62–72.

Wang C. and Tseng, Y. (2004). Dual-directional profilefilter for digital terrain model generation from airborne laser scanning data. *J. Appl. Remote Sens.* 2014;8:4480–4494. doi: 10.1117/1.JRS.8.083619.

Wehr, A. and Lohr, U. (1999). Airborne Laser Scanning - An Introduction and Overview. *ISPRS Journal of Photogrammetry & Remote Sensing*, 54, pp. 68 - 82.

Yastikli, N. and Cetin, Z. (2016). Classification of LiDAR Data with Point Based Classification Methods, *Int. Arch. Photogramm. Remote Sens. Spatial Inf. Sci.*, XLI-B3, 441-445, doi:10.5194/isprs-archives-XLI-B3-441-2016.

Zhang, K. and Chen, S.C. (2003). A progressive morphological filter for removing nonground measurements from airborne LiDAR data. *IEEE Transactions on Geoscience and Remote Sensing* 41, pp. 872–882.

Zhou, Q. Y. and Neumann, U. (2008). Fast and extensible building modeling from airborne LiDAR data. Proceedings of the 16th ACM SIGSPATIAL international conference on Advances in geographic information systems (on CD–ROM).

Cite this article as:
Makinde E. O. and Onaneye A.O. 2021. 3D City Model from LiDAR of Akoka, Lagos Using Geographical Information Technique. *Nigerian Journal of Environmental Sciences and Technology*, 6(1), pp. 180-192. https://doi.org/10.36263/nijest.2022.01.0292